

Assessing recent thaw and subsidence of peatland permafrost in coastal Labrador, northeastern Canada

Yifeng Wang¹

Robert G. Way¹

Antoni G. Lewkowicz²

Rosamond Tutton¹

Jordan Beer¹

Victoria Colyn¹

Anika Forget¹

¹Northern Environmental Geoscience Laboratory, Department of Geography and Planning, Queen's University. Corresponding author: yifeng.wang@queensu.ca

²Department of Geography, Environment and Geomatics, University of Ottawa.

This manuscript has undergone one round of peer-review for the Proceedings for the 12th International Conference on Permafrost in June 2024. Please feel free to contact the corresponding author with any questions or feedback.

ABSTRACT

Ground temperatures have been monitored since 2014 in four shallow boreholes (up to 5.7 m deep) drilled in palsas along the southeastern Labrador Sea coastline. This borehole network is critical for monitoring the effects of climate change on the terrestrial cryosphere and includes some of the southernmost coastal permafrost in the Northern Hemisphere. In this region, there are very few published measurements of active layer thickness, permafrost thickness, and permafrost temperatures. Mean annual ground temperatures of -1.7 to -0.7°C at 1 m depth were surprisingly low at the beginning of the study period, given the relatively thin bodies of permafrost present (<3 m thick). Statistically significant increases in ground temperatures were observed from 2015 to 2022 at some but not all depths in the four boreholes, despite decreases in permafrost thickness observed at all sites. Permafrost thaw resulted from both increased thaw penetration and thaw from the base of permafrost. Thaw penetration relative to the original ground surface increased by 24 to 92% due to a combination of active layer thickening and ground subsidence. Permafrost thaw at these sensitive locations may be driven by changes in mean annual air temperature, vegetation, snow dynamics, hydrology, and human disturbance. These data provide novel insights into the sensitivity of permafrost in this understudied region and can be used to validate predictive thermal modelling under future climate scenarios.

INTRODUCTION

Permafrost is typically present at high latitudes and/or at high elevations where mean annual air temperatures (MAAT) are usually below 0°C . Monitoring of ground temperatures in boreholes is fundamental to understanding changes in permafrost conditions (Noetzli et al. 2021, Isaksen et al. 2022). For the past several decades, permafrost temperatures have been compiled within the Global Terrestrial Network for Permafrost, and analyses of long-term permafrost borehole records have identified global increases in mean annual ground temperatures (MAGT) (Biskaborn et al. 2019). These temperature records are critical for understanding permafrost change, which can have impacts on related social, hydrological, and ecological systems (Walvoord and Kurylyk 2016, Schuur and Mack 2018, Gibson et al. 2021, Hjort et al. 2022).

Permafrost distribution in Labrador (Figure 1), northeastern Canada, ranges from continuous at high elevations and latitudes to discontinuous and isolated patches further south (Heginbottom et al. 1995). Recent investigations identified high densities of permafrost peatlands in lowland locations along the Labrador Sea coastline that contain palsas or peat plateaus (Wang et al. 2023). They extend as far south as 51.4°N and represent some of the most equatorward occurrences of coastal permafrost globally (Dionne 1984, Wang et al. 2023). Recent unmanned aerial vehicle-based analyses have revealed that these palsas and peat plateaus are small, fragmented, and highly vulnerable to thaw (Beer et al. 2023), and this is supported by historical aerial photograph analyses that show a rapid decline of peatland permafrost area in the region (Wang et al. 2024).

Despite advances in characterizing peatland permafrost in coastal Labrador, there remains a paucity of information on ground thermal conditions and permafrost thicknesses. To reduce these observational gaps, ground temperature monitoring was started in 2014 at four palsas located between 51.5°N and 53.7°N , forming part of the only active permafrost borehole monitoring network in Labrador (Figure 1). This paper summarizes the trends observed in thaw penetration and permafrost thickness and offers the first quantification of change in ground temperatures in permafrost environments in Labrador. This paper contributes to the advancement of knowledge on

permafrost as an Essential Climate Variable for the Global Climate Observing System (Smith and Brown 2009).

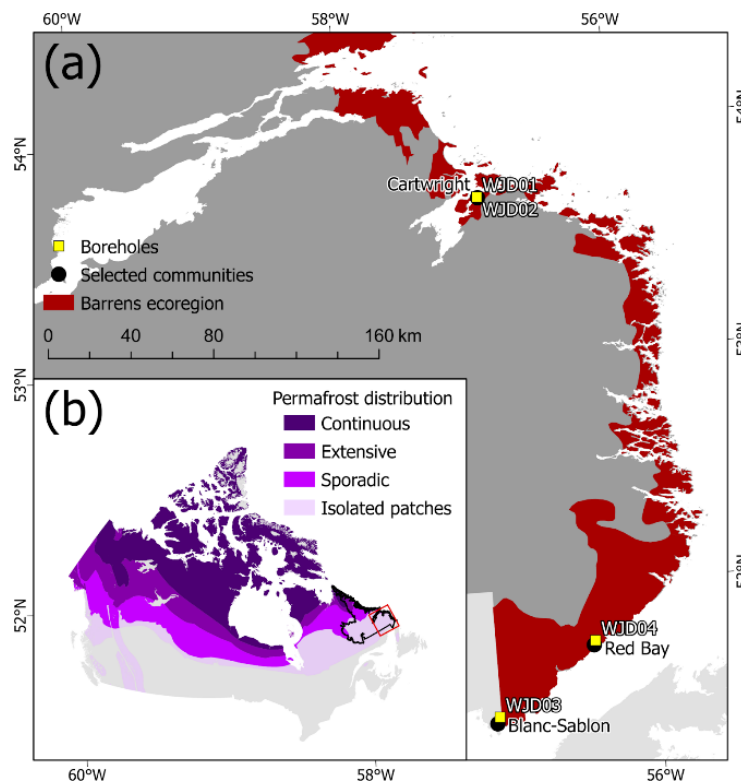


Figure 1. (a) Locations of palsa boreholes, selected communities, and the barrens ecoregion in southeastern coastal Labrador (Government of Newfoundland and Labrador 2020). (b) Inset map showing distribution of permafrost across Canada (Heginbottom et al. 1995) and location of Labrador.

STUDY AREA

Coastal Labrador experiences long, cold winters and short, cool summers and is strongly influenced by the cold Labrador Sea current that runs south along the coast (Banfield and Jacobs 1998, Roberts et al. 2006). MAATs generally decrease with latitude from 0.6°C at Blanc Sablon to 0.0°C at Cartwright, and to -2.5°C at the northernmost community of Nain, Nunatsiavut (56.5°N) (1981-2010 climate normal) (Environment and Climate Change Canada 2023), and have increased by $\sim 1.5^{\circ}\text{C}$ since 1881 (Way and Viau 2015). Coastal Labrador is also characterized by high amounts of precipitation (~ 1000 mm/year) (Hare 1950, Banfield and Jacobs 1998) with snow fractions of 0.37 for Blanc-Sablon, 0.43 for Cartwright, and 0.51 for Nain (1981-2010 climate normal) (Environment and Climate Change Canada 2023). Maximum snow depths occur in March, but high winds lead to significant snow redistribution across the coast's varying topography (Way and Lewkowicz 2018). Ecologically, much of coastal Labrador is classified as coastal barrens (Roberts et al. 2006), an ecosystem where trees are sparse due to a combination of both climatic and physiographic limitations (Figure 1). Wetlands are common (Mahdianpari et al. 2021), and peat thicknesses locally exceed 2 m (Séguin and Dionne 1992, Way et al. 2018). Peatland permafrost is especially concentrated in coastal lowland locations between 53°N and 55°N , where post-glacial marine incursion led to the deposition of fine-grained glaciomarine sediments (Hagedorn 2022, Wang et al. 2023). The region includes coastal portions of the Labrador Inuit

Settlement Area (Nunatsiavut) in the north, a land claims agreement-in-principle by the Innu Nation in central Labrador, and areas claimed by the NunatuKavut Community Council in the south that correspond to the region examined in this study.

The four monitoring boreholes are all on small palsas (Figure 2; Table 1). WJD01 and WJD02 are within the same peatland in the community of Cartwright. The palsas measured 0.49 and 0.52 m tall in 2021, and vegetation cover is intact and up to 30 and 3 cm high, respectively (Beer et al. 2023). This peatland is subject to high levels of human disturbance, as persistent snow drifting away from the palsa mounds has led to community members storing komatiks (Inuit style sleds) on palsa surfaces through the winter and over the summer. WJD03 is the southernmost borehole and is located in a 1.24 m high palsa near the community of Blanc-Sablon, Québec. Vegetation cover at this palsa is up to 12 cm high and is largely intact, with some patches of exposed peat found in lower parts of the mound (Beer et al. 2023). WJD04 is positioned on a 0.82 m high palsa near the community of Red Bay. Peat is exposed on the majority of the palsa and vegetation, where present, is up to 4 cm high (Beer et al. 2023).

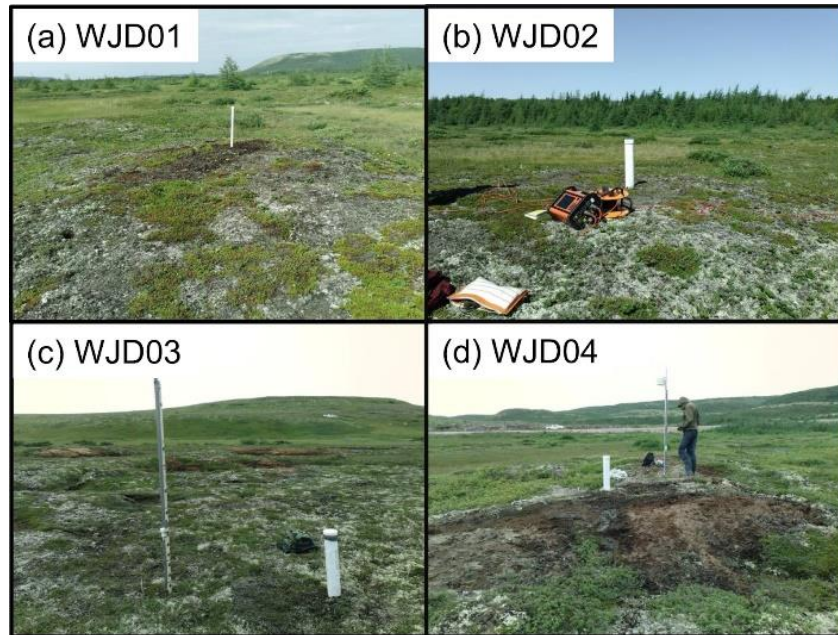


Figure 2. Field photos of the study boreholes and their surrounding conditions at the time of installation in 2014: (a) WJD01, (b) WJD02, (c) WJD03, and (d) WJD04.

Table 1. Characteristics of the coastal Labrador palsa boreholes.

| Borehole | Latitude (°N), Longitude (°W), Elevation (m asl) | Mean annual air temperature (°C) ¹ | Sensor depths (m) ² | Logger type ³ | Date established (YYYY-MM-DD) |
|----------|---|--|--------------------------------|-----------------------------|----------------------------------|
| WJD01 | 53.71, -57.01, 11 | 0.5 | 0.25, 0.5, 1, 2.15 | iB | 2014-07-23 |
| WJD02 | 53.71, -57.01, 14 | 0.5 | 0.5, 1.0, 2.0, 3.0, 4.25, 5.7 | Hobo | 2014-07-23 |
| WJD03 | 51.46, -57.12, 115 | 0.7 | 0.25, 0.5, 1.0, 2.0, 3.0, 4.2 | Hobo | 2014-08-05 |
| WJD04 | 51.76, -56.41, 75 | 1.1 | 0.25, 0.5, 1.0, 2.0, 3.0, 4.25 | Hobo | 2014-08-06 |

¹Mean annual air temperatures were aggregated from bi-hourly measurements taken by Hobo Pro v2 Temperature/Relative Humidity U23-001 loggers from adjacent meteorological monitoring stations. Mean annual air temperatures were calculated over hydrological years (October 1-September 30) from 2015-2016 to 2021-2022 (n=7).

²Note that sensor depths are relative to the ground surface at the time of installation in 2014.

³Hobo = Hobo V2 U23-003 loggers; iB = DS1922L High Resolution Thermochron F5 iButtons

METHODS

The four boreholes were drilled using the water jet technique in 2014, and the base of permafrost was reached and exceeded at three of the four locations (not at WJD01) (Way et al. 2018). Boreholes were cased with PVC pipe immediately after drilling and were instrumented at four to six depths with either Hobo V2 U23-003 loggers (accuracy $\pm 0.2^{\circ}\text{C}$; resolution $\pm 0.02^{\circ}\text{C}$ at 22°C but $>0.02^{\circ}\text{C}$ at 0°C), recording ground temperatures every 2 hours, or DS1922L High Resolution Thermochron F5 iButtons (accuracy $\pm 0.5^{\circ}\text{C}$; resolution $\pm 0.0625^{\circ}\text{C}$), recording ground temperatures every 4 hours (Table 1). Ground temperature records were interpolated to hourly increments using a spline and then aggregated to daily, monthly, and annual metrics for comparison between sites. Short data gaps in the ground temperature record at 5.7 m at WJD02 were infilled using cross-correlation between records from different depths in the same borehole (Way et al. 2018), but longer data gaps exist where loggers failed. Ground temperatures measured for one full hydrological year post-drilling were excluded to reduce the thermal impacts of disturbance during establishment (Way et al. 2018).

Thaw penetration depths were estimated by linearly extrapolating maximum annual ground temperatures to the depth corresponding to 0°C using measurements from two depths within the active layer over each hydrological year (October 1 to September 30) (Riseborough 2003, 2008). WJD02 lacked the two measurement depths in the active layer necessary for extrapolation, so measurements from a 0.25 m depth ground temperature logger located at an adjacent palsa monitoring station (AMET13) was used together with the existing 0.5 m measurement. The 0.25 m depth measurement from AMET13 was linearly scaled to better match WJD02 local site conditions using an equation ($y=1.3836x-0.2585$; $R^2=0.96$) derived from overlapping ~ 50 cm depth measurements at AMET13 and WJD02 over 2015-2016. Thaw penetration relative to the initial ground surface was considered instead of thaw depth from the current ground surface to account for the impacts of both active layer thickening and ground subsidence (O'Neill et al. 2023), which can occur simultaneously in ice-rich landforms, including palsas. Total subsidence at the borehole locations from the time of initial installation in Summer 2014 to the most recent field visit in Summer 2023 was calculated from the difference in the depths of the shallowest logger within the borehole casing relative to the ground surface between the two summers. The depths corresponding to the zero annual amplitude were identified from linear interpolation from minimum annual and maximum annual temperature curves, calculated over hydrological years (October 1 to September 30), where the range in minimum and maximum annual temperatures was less than 0.1°C . The depths corresponding to the base of permafrost were defined as the greatest depth where the maximum annual temperature curve, calculated over hydrological years (October 1 to September 30), intersected with 0°C ($\pm 0.04^{\circ}\text{C}$ to account for decreased logger resolution near 0°C).

RESULTS

Changes in thaw penetration and permafrost thickness

Thaw penetration in 2015-2016 was less than 1 m at all borehole locations, ranging from 0.53 to 0.85 m (Table 2; Figure 3). The depth of the base of permafrost exceeded 2.15 m and ranged up to 3.53 m, giving permafrost thicknesses of up to 2.92 m. Thaw penetration increased at all locations over the monitoring period (almost doubling at WJD01 and WJD02 to 1.01 and 1.02 m, respectively), and permafrost thicknesses decreased (to as little as 0.50 m at WJD01) (Table 2). The increase in thaw penetration represented 42 to 59% of the change in permafrost

thickness at the sites. Thaw from the base of permafrost also accounted for a substantial proportion of the change in permafrost thickness (41 to 58%) (Table 2). Total subsidence observed at the boreholes was 5 to 50 cm (Table 2), accounting for at least 10% of the increase in thaw penetration (O'Neill et al. 2023).

Changes in ground thermal regime

Considering the thin permafrost present at the borehole sites, mean ground temperatures in 2015-2016 were surprisingly low, varying from -0.7°C at a depth of 1 m at WJD04 to -1.7°C at a depth of 1 m at WJD02 (Figure 3). The range in ground temperatures was up to $\sim 25^{\circ}\text{C}$ at the shallowest depth of 0.25 m (Figure 3), but decreased rapidly with depth at all sites, with depths of zero annual amplitude declining from 4.1 m in 2015-2016 to 2.9 m in 2021-2022 (Table 2).

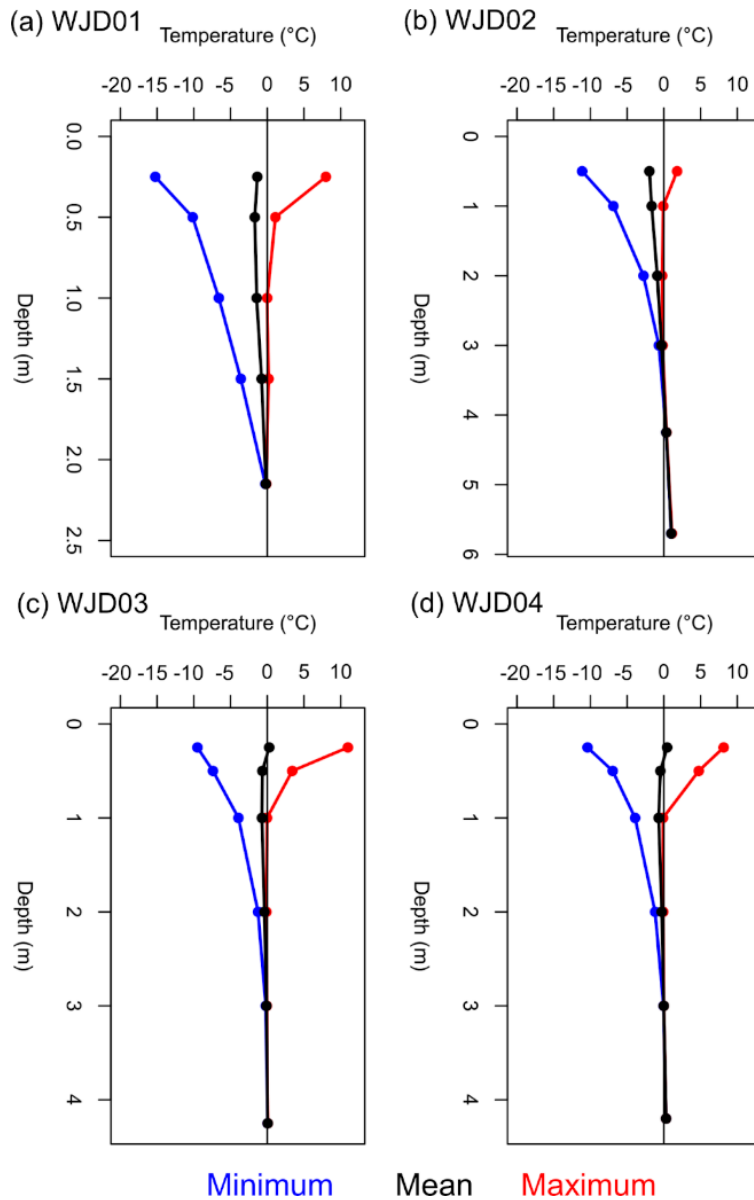


Figure 3. Minimum, mean, and maximum ground thermal profiles for (a) WJD01, (b) WJD02, (c) WJD03, and (d) WJD04 for October 2015 to September 2016 (Oct-Sept). Note that the depths on the y axes are scaled according to the depth of each borehole.

Table 2. Summary of permafrost characteristics at the palsa boreholes for the earliest (2015-2016) and most recent hydrological years of record (2021-2022). Depths of thaw penetration, base of permafrost, and zero annual amplitude are relative to the initial ground surface at the time of installation in 2014.

| Borehole | 2015-2016 | | | | 2021-2022 | | | 2014-2023 | |
|----------|----------------------------|---------------------------------|--------------------------|------------------------------------|----------------------------|---------------------------------|--------------------------|------------------------------------|----------------|
| | Thaw penetration depth (m) | Depth of base of permafrost (m) | Permafrost thickness (m) | Depth of zero annual amplitude (m) | Thaw penetration depth (m) | Depth of base of permafrost (m) | Permafrost thickness (m) | Depth of zero annual amplitude (m) | Subsidence (m) |
| WJD01 | 0.54 | >2.15 | >1.61 | >2.15 | 1.01 | 1.51 | 0.50 | 2.09 | 0.05 |
| WJD02 | 0.53 | 3.39 | 2.86 | 4.11 | 1.02 | 3.05 | 2.03 | 2.88 | 0.50 |
| WJD03 | 0.61 | 3.53 | 2.92 | 3.44 | 1.00 | 3.26 | 2.26 | 1.92 | 0.12 |
| WJD04 | 0.85 | 3.30 | 2.45 | 2.90 | 1.05 | 3.04 | 1.99 | 2.30 | 0.40 |

Mean ground temperatures increased through the monitoring period (Figure 4), but not monotonically (Figure 5). Exceptionally high ground temperatures were observed at all locations in 2020-2021 in response to anomalously warm air temperatures, which were 2.2-2.5°C warmer than the annual average for 2015-2020. Supra-permafrost taliks were not observed at any of the sites, and ground conditions cooled slightly in the following year (2021-2022) (Figure 4; Figure 5). Statistically significant ground temperature warming was observed within the permafrost at WJD01, at all depths at WJD02, beneath the permafrost at WJD03, and both above and beneath the permafrost at WJD04 (Figure 6).

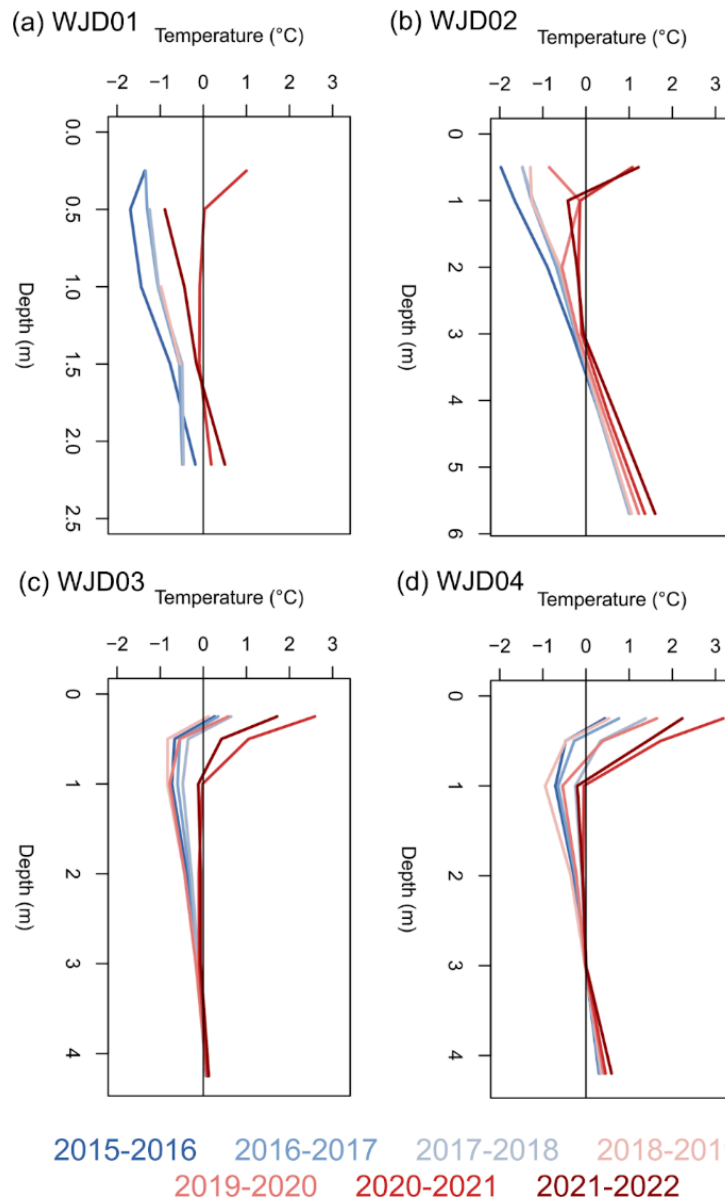


Figure 4. Mean annual ground temperature profiles at (a) WJD01, (b) WJD02, (c) WJD03, and (d) WJD04 from 2015-2016 to 2021-2022. Mean annual ground temperatures were calculated over hydrological years (October 1-September 30). Note that the depths on the y axes are scaled according to the depth of each borehole.

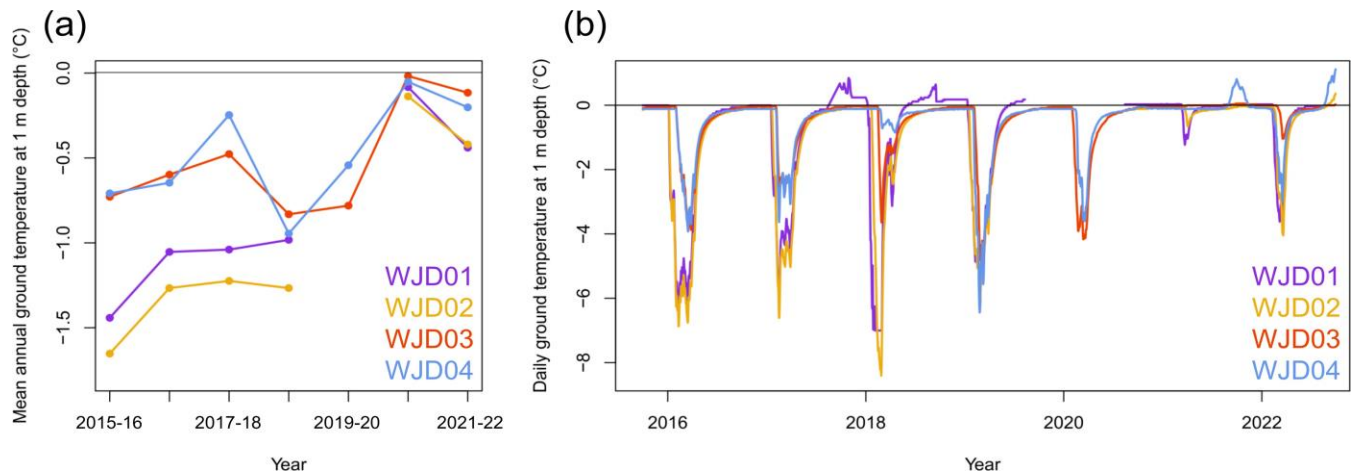


Figure 5. Mean (a) annual and (b) daily ground temperatures at a depth of 1 m at WJD01, WJD02, WJD03, and WJD04 from 2015-2022. Horizontal black lines represent 0°C.

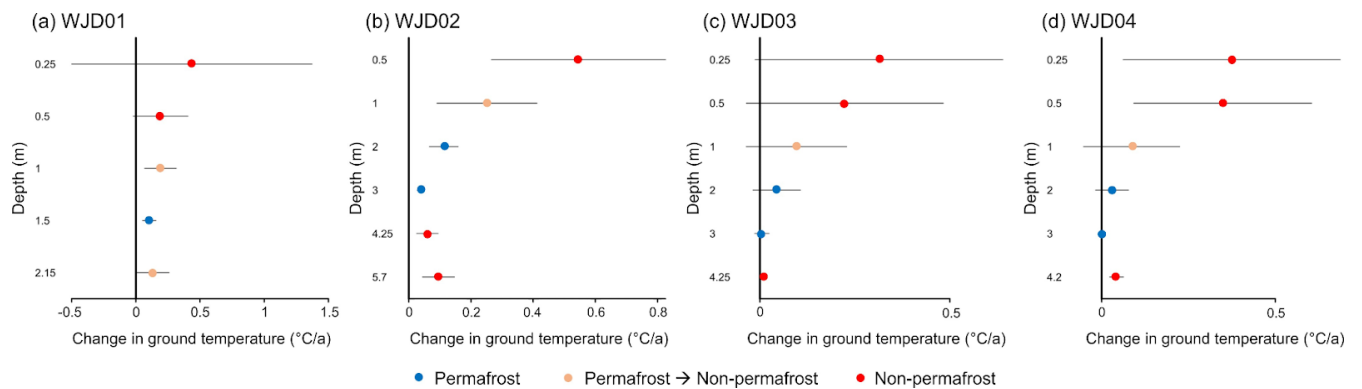


Figure 6. Summary of linear trends in mean annual ground temperatures at (a) WJD01, (b) WJD02, (c) WJD03, and (d) WJD04 from 2015-2016 to 2021-2022. Mean annual ground temperatures were calculated over hydrological years (October 1-September 30). Horizontal black lines represent 95% confidence intervals.

DISCUSSION

Thaw and subsidence of peatland permafrost in coastal Labrador

The coastal Labrador palsa monitoring network has helped to characterize the thermal conditions of thin, yet surprisingly cold, bodies of permafrost along the southeastern Labrador Sea coastline. The combination of relatively low temperatures but limited permafrost thickness has been attributed to lateral heat flow from the surrounding non-permafrost area, possibly combined with advective heat fluxes due to groundwater flow beneath the mounds (Osterkamp 2003, Way et al. 2018).

Monitoring of ground temperatures at the four boreholes shows increasing thaw penetration and permafrost thaw since installation in 2014. Warming occurred at all sites, but rates were not statistically significant at all depths in all boreholes. Inter-borehole differences may be attributed to variations in site characteristics, including vegetation cover, peat thickness, underlying sediment type and texture, hydrological connectivity, and human disturbance (Thie 1974, Allard and Rousseau 1999, Zuidhoff and Kolstrup 2005). For example, higher vegetation heights at WJD01 and the placement of komatiks by community members near WJD01 and WJD02, could lead to greater snow trapping and reduced energy escape from the ground in winter, while the thicker

snow could also increase surface moisture during snowmelt. At WJD04, vegetation cover has mostly disappeared through processes of degradation and deflation, such that the top of the palsa is mostly characterized by exposed peat. As a result, the palsa at WJD04 likely has a lower albedo and different moisture characteristics compared to the other three sites.

Mechanisms of permafrost thaw were similar across all four locations, with a combination of thaw from both the bottom and top of permafrost. Thaw from the base of permafrost, which occurred by 27 to 64 cm, was likely caused by increased energy fluxes from the warmer surrounding unfrozen wetland and by water around and/or beneath the thin bodies of permafrost (Osterkamp 2003). Thaw from the top of permafrost is more complicated, as increases in thaw penetration occurred as a result of both active layer thickening and ground subsidence (O'Neill et al. 2023). By taking measurements of the borehole sensor depths relative to the surrounding ground surface in Summer 2023, the amount of subsidence could be estimated for each borehole since 2014 (Figure 7). In the absence of more precise measurement techniques, such as using a differential GPS to measure changes in the elevation of the ground surface from year to year, this comparative technique provides a reasonable approximation of the subsidence that occurred in the surrounding palsa at each borehole. This estimate then allowed us to differentiate between the proportion of thaw penetration as subsidence (5 to 50 cm, 11 to 200%) versus the proportion of thaw penetration as active layer thickening. This varied between sites, with 11% occurring as subsidence and 89% occurring as active layer thickening at WJD01 and 31% occurring as subsidence and 69% occurring as active layer thickening at WJD03. This likely reflects differences in ground ice content between the landforms at WJD01 and WJD03, as permafrost with higher ground ice content is expected to have greater potential for subsidence as it thaws, while permafrost with lower ground ice content may experience change in a more subtle manner (Kokelj and Jorgenson 2013, Olefeldt et al. 2016). At WJD02 and WJD04, the amount of subsidence measured in Summer 2023 relative to Summer 2014 exceeded the total thaw penetration that was calculated for the study period. This may reflect potential changes in buoyancy within the wetland (Seppälä 1994), frost heave and jacking of the borehole casing itself, or limitations in using loggers (i.e., accuracy, resolution) when monitoring permafrost temperatures close to 0°C.

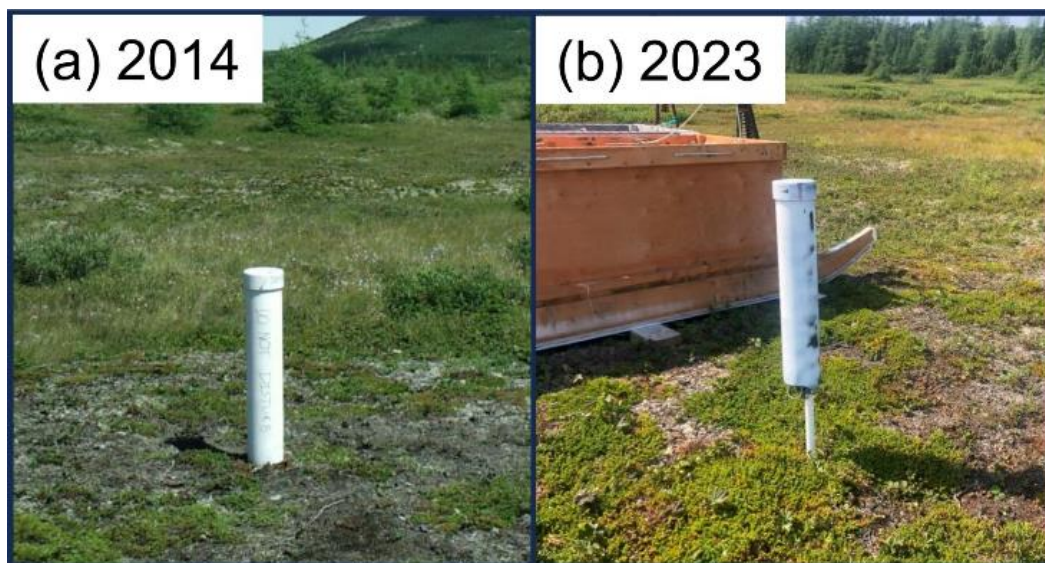


Figure 7. Field photos of WJD02 in (a) 2014 and (b) 2023. Since 2014, residents of the nearby community of Cartwright have parked a komatik on the WJD02 palsa. There was also visually evident subsidence at this site between 2014 and 2023.

Enhanced thaw, manifested as both active layer thickening and subsidence, occurred in Summer 2021, following an exceptionally warm winter (+5°C higher than the baseline average for 1961-1990) (Environment and Climate Change Canada 2021) in coastal Labrador in 2020-2021. Summer 2021 was the first time that ground temperatures at a nominal depth of 1 m at WJD03 and WJD04 exceeded 0°C, while ground temperatures at 1 m depth at WJD01 and WJD02 were right at the point of thaw (Figure 5), thus we hypothesize that most of the observed ground subsidence occurred that year. Ground temperatures returned to slightly lower values in Winter 2021-2022. Continued monitoring of these landforms will be critical to understanding the long-term impacts of extreme winter events like 2020-2021 on peatland permafrost in the region.

Possible limitations

Differences in patterns and mechanisms of permafrost thaw between WJD01 and the other three palsa boreholes, especially with WJD02 located only 60 m away, may be potentially due to the sensitivity and accuracy of the data loggers that were used. As WJD01 is instrumented with less accurate DS1922L High Resolution Thermochron F5 iButtons (accuracy $\pm 0.5^\circ\text{C}$; resolution $\pm 0.0625^\circ\text{C}$) compared to Hobo V2 U23-003 loggers (accuracy $\pm 0.2^\circ\text{C}$; resolution $\pm 0.02^\circ\text{C}$ at 22°C but $>0.02^\circ\text{C}$ at 0°C), it is possible that ground temperatures at WJD01 are lower than recorded and that permafrost is thicker than presented here (Table 2). Additional investigations, such as geophysical surveys (Way et al. 2018), may help resolve the interpretation of permafrost thickness at this location.

Estimates of thaw penetration were especially challenging for WJD02 due to the arrangement of the temperature loggers at this borehole. While it was possible in this case to estimate the ground temperature at 25 cm at WJD02 for 2015-2016 based on an overlapping record at an adjacent monitoring location (AMET13), a closer spacing of thermistors at the boreholes, especially within the active layer, will be needed to assess ongoing and future changes in thaw penetration.

Other boreholes in the region

The only other palsa borehole in this region of northeastern Canada is located ~5 km north of WJD03 at 51.50°N, 57.15°W. Ground temperatures at this borehole from 2004-2005 to 2011-2012 were near 0°C (MAGT of -0.46°C at 1 m), and temperature records showed consistent active layer thicknesses just under 1 m and a base of permafrost deeper than 10 m throughout the study period (Centre d'études nordiques 2013). This borehole experienced statistically significant warming at 4 m by 0.02°C/year from 2004 to 2012 and simultaneous statistically significant cooling at 5, 6, 9, and 10 m by up to -0.29°C/year. This temperature record unfortunately does not overlap temporally with our four borehole records, and it does not reflect significant changes in air temperature, vegetation, and snow that have occurred in the region since 2012 (Barrette et al. 2020, Wang et al. 2024). The continued monitoring of existing permafrost landforms and the expansion and installation of new boreholes in other peatland permafrost landforms in the region will be essential for characterizing permafrost change in the context of a warming climate.

CONCLUSION

Borehole records reveal progressive thaw at four palsa sites in coastal Labrador from 2015 to 2022. Thermal changes were subtle, as is characteristic of permafrost that is close to 0°C (Smith et al. 2005), but when coupled with apparent physical changes, these data show ongoing increases

in thaw penetration and declines in permafrost thickness. Permafrost thickness decreased by 18 to 69%, while thaw penetration increased by 24 to 92%. Thaw penetration was found to be attributed to a combination of active layer thickening and ground subsidence, and differences in the proportion of active layer thickening versus ground subsidence may reflect variations in ground ice content between palsas. Six additional boreholes, drilled in palsas (n=4) and peat plateaus (n=2) from 2015 to 2022 via water jet or percussive drilling techniques, will supplement this existing dataset and provide additional context for ground thermal conditions in peatland permafrost landforms found as far north as 56.6°N in coastal Labrador.

ACKNOWLEDGEMENTS

The coastal Labrador peatland permafrost borehole monitoring network is located across the traditional lands of Labrador Inuit, Innu, and Kallunângajuit. Research permits for work conducted at WJD01-04 were granted by the NunatuKavut Community Council Research Advisory Committee, and we are grateful to Bryn Wood, George Russell Jr., Charlene Kippenhuck, and Meredith Purcell, as well as the residents of Cartwright and Red Bay, for their support. We are also grateful to George Russell Jr., Lloyd Pardy, and Gary Bird for meaningful and insightful conversations about peatland permafrost change in southeastern coastal Labrador that helped to motivate this research. Funding for this research was provided by the Natural Sciences and Engineering Research Council of Canada, the Northern Scientific Training Program, Queen's University, the University of Ottawa, the Weston Family Foundation, and the Association of Canadian Universities for Northern Studies. We thank Sharon Smith and Brendan O'Neill for helpful discussions about thaw penetration, and we thank the editor and two anonymous reviewers for their helpful and constructive commentary on this manuscript.

REFERENCES

- Allard, M., and Rousseau, L. 1999. The international structure of a palsa and a peat plateau in the Rivière Boniface region, Québec: Inferences on the formation of ice segregation mounds. *Géographie physique et Quaternaire*, **53**(3): 373–387. doi:10.7202/004760ar.
- Banfield, C.E., and Jacobs, J.D. 1998. Regional patterns of temperature and precipitation for Newfoundland and Labrador during the past century. *The Canadian Geographer/Le Géographe canadien*, **42**(4): 354–64. doi:10.1111/j.1541-0064.1998.tb01351.x.
- Barrette, C., Brown, R., Way, R.G., Mailhot, A., Diaconescu, E.P., Grenier, P., Chaumont, D., Dumont, D., Sévigny, C., Howell, S., and Senneville, S. 2020. Nunavik and Nunatsiavut regional climate information update. *In Nunavik and Nunatsiavut: From science to policy, an integrated regional impact study (IRIS) of climate change and modernization, second iteration. Edited by P. Ropars, M. Allard, and M. Lemay. ArcticNet Inc., Quebec City, Canada. p. 62.*
- Beer, J., Wang, Y., Way, R.G., Forget, A., and Colyn, V. 2023. Uncrewed aerial vehicle-based assessments of peatland permafrost resiliency along the Labrador Sea coastline, northern Canada (Preprint). *EarthArXiv*,. doi:10.31223/X5610M.
- Biskaborn, B.K., Smith, S.L., Noetzli, J., Matthes, H., Vieira, G., Streletskiy, D.A., Schoeneich, P., Romanovsky, V.E., Lewkowicz, A.G., Abramov, A., Allard, M., Boike, J., Cable, W.L., Christiansen, H.H., Delaloye, R., Diekmann, B., Drozdov, D., Etzelmüller, B., Grosse, G., Guglielmin, M., Ingeman-Nielsen, T., Isaksen, K., Ishikawa, M., Johansson, M., Johansson, H., Joo, A., Kaverin, D., Kholodov, A., Konstantinov, P., Kröger, T.,

- Lambiel, C., Lanckman, J.-P., Luo, D., Malkova, G., Meiklejohn, I., Moskalenko, N., Oliva, M., Phillips, M., Ramos, M., Sannel, A.B.K., Sergeev, D., Seybold, C., Skryabin, P., Vasiliev, A., Wu, Q., Yoshikawa, K., Zheleznyak, M., and Lantuit, H. 2019. Permafrost is warming at a global scale. *Nature Communications*, **10**(1): 264. doi:10.1038/s41467-018-08240-4.
- Centre d'études nordiques. 2013. Données environnementales de la station Blanc-Sablon, Québec, Canada, v. 1.0 (1990-2012). Nordicana D5,. doi:10.5885/45111SL-B5D073186F274136.
- Dionne, J.-C. 1984. Paleses et limite méridionale du pergélisol dans l'hémisphère nord : Le cas de Blanc-Sablon, Québec. *Géographie physique et Quaternaire*, **38**(2): 165–184. doi:10.7202/032550ar.
- Environment and Climate Change Canada. 2021. Winter 2020/2021. https://publications.gc.ca/collections/collection_2021/eccc/En81-23-2021-1-eng.pdf.
- Environment and Climate Change Canada. 2023. Canadian climate normals. https://climate.weather.gc.ca/climate_normals/index_e.html.
- Gibson, C., Cottenie, K., Gingras-Hill, T., Kokelj, S.V., Baltzer, J.L., Chasmer, L., and Turetsky, M.R. 2021. Mapping and understanding the vulnerability of northern peatlands to permafrost thaw at scales relevant to community adaptation planning. *Environmental Research Letters*, **16**(5): 055022. doi:10.1088/1748-9326/abe74b.
- Government of Newfoundland and Labrador. 2020. Labrador ecoregions. <https://geohub-gnl.hub.arcgis.com/datasets/labrador-ecoregions/explore>.
- Hagedorn, G.W. 2022. Preliminary delineation of marine sediments in east-central Labrador: Parts of NTS map areas 13F, -G, -I, -J, -K, -N AND -O. Government of Newfoundland and Labrador, Department of Industry, Energy and Technology Current Research, **22**(1): 189–201. https://www.gov.nl.ca/iet/files/CurrentResearch_Hagedorn_2022.pdf.
- Hare, F.K. 1950. Climate and zonal divisions of the boreal forest formation in eastern Canada. *Geographical Review*, **40**(4): 615. doi:10.2307/211106.
- Heginbottom, J.A., Dubreuil, M.A., and Harker, P.T. 1995. Canada, Permafrost. National Atlas of Canada, Natural Resources Canada, Geomatics Canada, <https://doi.org/10.4095/294672>.
- Hjort, J., Streletskiy, D., Dore, G., Wu, Q., Bjella, K., and Luoto, M. 2022. Impacts of permafrost degradation on infrastructure. *Nature Reviews Earth & Environment*, **3**: 24–38. doi:10.1038/s43017-021-00247-8.
- Isaksen, K., Lutz, J., Sørensen, A.M., Godøy, Ø., Ferrighi, L., Eastwood, S., and Aaboe, S. 2022. Advances in operational permafrost monitoring on Svalbard and in Norway. *Environmental Research Letters*, **17**(9): 095012. doi:10.1088/1748-9326/ac8e1c.
- Kokelj, S.V., and Jorgenson, M.T. 2013. Advances in thermokarst research. *Permafrost and Periglacial Processes*, **24**(2): 108–119. doi:10.1002/ppp.1779.
- Mahdianpari, M., Brisco, B., Granger, J., Mohammadimanesh, F., Salehi, B., Homayouni, S., and Bourgeau-Chavez, L. 2021. The third generation of pan-Canadian wetland map at 10 m resolution using multisource earth observation data on cloud computing platform. *IEEE Journal of Selected Topics in Applied Earth Observations and Remote Sensing*, **14**: 8789–8803. doi:10.1109/JSTARS.2021.3105645.
- Noetzli, J., Arenson, L.U., Bast, A., Beutel, J., Delaloye, R., Farinotti, D., Gruber, S., Gubler, H., Haerberli, W., Hasler, A., Hauck, C., Hiller, M., Hoelzle, M., Lambiel, C., Pellet, C.,

- Springman, S.M., Vonder Muehll, D., and Phillips, M. 2021. Best practice for measuring permafrost temperature in boreholes based on the experience in the Swiss Alps. *Frontiers in Earth Science*, **9**: 607875. doi:10.3389/feart.2021.607875.
- Olefeldt, D., Goswami, S., Grosse, G., Hayes, D., Hugelius, G., Kuhry, P., McGuire, A.D., Romanovsky, V.E., Sannel, A.B.K., Schuur, E.A.G., and Turetsky, M.R. 2016. Circumpolar distribution and carbon storage of thermokarst landscapes. *Nature Communications*, **7**(1): 13043. doi:10.1038/ncomms13043.
- O'Neill, H.B., Smith, S.L., Burn, C.R., Duchesne, C., and Zhang, Y. 2023. Widespread permafrost degradation and thaw subsidence in northwest Canada. *Journal of Geophysical Research: Earth Surface*, **128**(8): e2023JF007262. doi:10.1029/2023JF007262.
- Osterkamp, T.E. 2003. A thermal history of permafrost in Alaska. *Proceedings of the 8th International Conference on Permafrost*,: 863–868.
- Riseborough, D.W. 2003. Thawing and freezing indices in the active layer. *Proceedings of the 8th International Conference on Permafrost*,: 953–958.
- Riseborough, D.W. 2008. Estimating active layer and talik thickness from temperature data: Implications from modelling results. *Proceedings of the 9th International Conference on Permafrost*,: 1487–1492.
- Roberts, B.A., Simon, N.P.P., and Deering, K.W. 2006. The forests and woodlands of Labrador, Canada: Ecology, distribution and future management. *Ecological Research*, **21**(6): 868–880. doi:10.1007/s11284-006-0051-7.
- Schuur, E.A.G., and Mack, M.C. 2018. Ecological response to permafrost thaw and consequences for local and global ecosystem services. *Annual Review of Ecology, Evolution, and Systematics*, **49**(1): 279–301. doi:10.1146/annurev-ecolsys-121415-032349.
- Séguin, M.K., and Dionne, J.C. 1992. Modélisation géophysique et caractérisation thermique du pergélisol dans les paises de Blanc-Sablon, Quebec. *Geological Survey of Canada Current Research*, **E**(1): 207–216. doi:10.4095/133575.
- Seppälä, M. 1994. Snow depth controls palsa growth. *Permafrost and Periglacial Processes*, **5**(4): 283–288. doi:10.1002/ppp.3430050407.
- Smith, S.L., and Brown, J. 2009. Assessment of the status of the development of the standards for the Terrestrial Essential Climate Variables: Permafrost and seasonally frozen ground. *Global Terrestrial Observing System*.
<https://globalcryospherewatch.org/bestpractices/docs/GTOS62.pdf>.
- Smith, S.L., Burgess, M.M., Riseborough, D., and Mark Nixon, F. 2005. Recent trends from Canadian permafrost thermal monitoring network sites. *Permafrost and Periglacial Processes*, **16**(1): 19–30. doi:10.1002/ppp.511.
- Thie, J. 1974. Distribution and thawing of permafrost in the southern part of the discontinuous permafrost zone in Manitoba. *ARCTIC*, **27**(3): 189–200. doi:10.14430/arctic2873.
- Walvoord, M.A., and Kurylyk, B.L. 2016. Hydrologic impacts of thawing permafrost—A review. *Vadose Zone Journal*, **15**(6): 1–20. doi:10.2136/vzj2016.01.0010.
- Wang, Y., Way, R.G., and Beer, J. 2024. Multi-decadal degradation and fragmentation of palsas and peat plateaus in coastal Labrador, northeastern Canada. *Environmental Research Letters*, **19**(1): 014009. doi:10.1088/1748-9326/ad0138.

- Wang, Y., Way, R.G., Beer, J., Forget, A., Tutton, R., and Purcell, M.C. 2023. Significant underestimation of peatland permafrost along the Labrador Sea coastline in northern Canada. *The Cryosphere*, **17**(1): 63–78. doi:10.5194/tc-17-63-2023.
- Way, R.G., and Lewkowicz, A.G. 2018. Environmental controls on ground temperature and permafrost in Labrador, northeast Canada. *Permafrost and Periglacial Processes*, **29**(2): 73–85. doi:10.1002/ppp.1972.
- Way, R.G., Lewkowicz, A.G., and Zhang, Y. 2018. Characteristics and fate of isolated permafrost patches in coastal Labrador, Canada. *The Cryosphere*, **12**(8): 2667–2688. doi:10.5194/tc-12-2667-2018.
- Way, R.G., and Viau, A.E. 2015. Natural and forced air temperature variability in the Labrador region of Canada during the past century. *Theoretical and Applied Climatology*, **121**(3–4): 413–424. doi:10.1007/s00704-014-1248-2.
- Zuidhoff, F.S., and Kolstrup, E. 2005. Palsa development and associated vegetation in northern Sweden. *Arctic, Antarctic, and Alpine Research*, **37**(1): 49–60. doi:10.1657/1523-0430(2005)037[0049:PDAAVI]2.0.CO;2.